Analytic reconstruction with algebraically trained filters for limited-angle tomography

Seungjun Yoo[a], Seokwon Oh[a], Junho Lee[a], and Ho Kyung Kim [a,*]
[a] *Radiation Imaging Laboratory, School of Mechanical Engineering, Pusan Nat'l Univ., Busandaehakro 63beon-gil, Busan 46241*
[*] *Corresponding author: hokyung@pusan.ac.kr*

***Keywords : Computed tomography, Limited-angle tomography, Algebraic filter, Out-of-plane artifact**

1. Introduction

While medical X-ray computed tomography (CT) pays concern to the patient dose, the main concerns in industrial CT for mass production are tube heat load and scan speed, considering production throughput. Recently, CT has been widely accepted for inspecting advanced parts such as printed circuit boards (PCBs) and lithium-ion batteries [1]. Given the need for high-speed projection data acquisition and the small aspect ratio of object geometry, CT scans with smaller angular ranges of less than 180°, known as limited angle tomography (LAT), are popular. The time required for image reconstruction from the acquired projections is also a crucial factor in determining inspection speed in industrial CT.

The analytical reconstruction algorithm, such as filtered backprojection (FBP), is the fastest. However, it is prone to provoke artifacts [2, 3], such as out-of-plane artifacts and halo artifacts, especially when the projections are noisy, sampled sparsely or irregularly across the scanning angle, or acquired over an angle less than 180°. This is because FBP finds an analytical solution by assuming a continuous representation of the image reconstruction problem. Iterative reconstruction (IR) methods have the advantage of reducing artifacts and noise, but their main drawback is the high computational complexity and cost, which presents a barrier to the adoption of IR in industrial CT.

In this study, to incorporate the properties of IR into FBP, algebraic filters trained by the Landweber algorithm are adopted for LAT. Subsequently, the performance of FBP with the algebraic filter (aFBP) applied to LAT is evaluated.

2. Methods and Materials

2.1 Theoretical background

IR methods find approximate solutions from discretized images: $A\mathbf{x} = \mathbf{b}$, where $\mathbf{x}$ and $\mathbf{b}$ are discretized versions of the image to be reconstructed and the projection data, respectively, and A represents the system metrix mapping the image to the projection. We may find a solution by minimizing $\|A\mathbf{x} - \mathbf{b}\|$. Using the objective function, including a regularizer (R), many iterative minimization alogrithms can be expressed as [4]:

$$\mathbf{x}^{k+1} = \mathbf{x}^k + \alpha[A^T W(\mathbf{b} - A\mathbf{x}^k) - \beta R\mathbf{x}^k], \quad (1)$$

where α and β are relaxation and regularization parameters, respectively, and W is an algorithm-dependent square matrix. With some mathematical manipualtions, this recursive form can be expressed as the closed form as:

$$\mathbf{x}^{k+1} = FA^T W\mathbf{x}^k. \quad (2)$$

Where F is the filtering matrix and can be expressed as follows:

$$F = (A^T WA + \beta R)^{-1}[I - (I - \alpha A^T WA - \alpha\beta R)^k]. \quad (3)$$

This study aims to incorporate IR properties into the FBP, achieving fast reconsturction with limited data. If $W = I$ in the above equation, we may regard that the $(k+1)$-th IR solution as equivalent to the filtered version of the backprojected k-th solution. The filtering matrix F is a function of IR parameters, i.e. α, β, and k. This study seeks F in the spatial frequency domain to implement it as a filter function in FBP, therby reducing the artifacts.

2.2 Evalution

To quantify the out-of-plane artifact, artifact-spread function (ASF) and its half-width at half-maximum (HWHM) are evaluated using an aluminum (Al) disc phantom. The ASF can be defined as a ratio of contrasts of the Al disc at the central slice (z = 0 mm) and other slices.

$$\mathrm{ASF}(z) = \frac{\Delta\mu(z)}{\Delta\mu(z)|_{z=0}}, \quad (4)$$

where $\Delta\mu(z)$ denotes the contrast of the Al disc.

Projection data according to the scan angle θ are acquired using a bench-top CBCT system. A tungsten target X-ray tube (XTF5011, Oxford Instruments, Oxfordshire, UK) emits a 45 kVp spectrum, and a 1548 × 1032 formatted X-ray detector (Shad-o-Box 1548 HS, Teledyne Rad-icon Imaging Corp., Sunnyvale, CA) with a pixel pitch of 99 μm is used for image acquisition. Additionally, under the same experimental conditions, a qualitative evaluation is conducted on a PCB sample for more practical application.

3. Preliminary Results

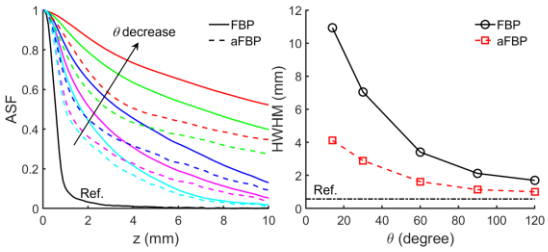

Fig. 1. ASFs as a function of depth z with respect to the scan angle θ, and there HWHMs as a function of the scan angle θ. The reference reconstructed from the full-scan FBP.

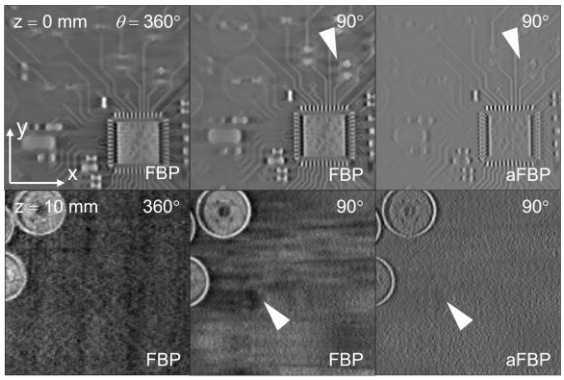

Fig. 2. The PCB sample images ($x-y$ plane images) reconstructed at different depths. The first and second rows correspond to reconstructions at z = 0 and 10 mm, respectively. The scan angle θ and the used reconstruction method are indicated in the top-right corner and bottom-right corners of each image, respectively.

Fig. 1 shows the ASFs and their HWHMs as a function of the scan angle θ. For FBP, the Hann-window function was used for filtering, while for aFBP, Eq. (3) was applied to the FBP filtering instead of the Hann-window function. As with full (θ = 360°)-scan FBP, since the thickness of the Al disc is 1 mm, the value of ASF should drop to 0 from z = 0 mm; otherwise, it can be considered that the out-of-plane artifact occur to a ghost by the Al disc. As θ decreased, the out-of-plane artifact became more pronounced, and the degradation in depth resolution due to ghosting was less severe in aFBP compared to FBP. Similarly, the HWHM of aFBP as a function of scan angle decreased by more than 50% compared to that of FBP.

Fig. 2 shows the slice images according to the filtering function, with the full-scan FBP included for comparison. At z = 0 mm, FBP shows a halo artifact in the highly attenuated metal region, whereas this artifact is reduced in the case of aFBP (see white arrows). Additionally, at z = 10 mm, the background region of the FBP slice image appears lumpy due to the influence of ghosting from other layers. In contrast, aFBP shows a uniform background region with reduced ghosting effects, although there appears to be a slight increase in high-frequency noise.

4. Conclusion

To reduce artifacts caused by insufficient angular data in LAT, an algebraic filter derived from the IR method was introduced. As shown in the ASF results, the proposed method (aFBP) was able to reduce the out-of-plane artifacts compared to conventional methods (FBP). Furthermore, qualitative evaluations of the PCB sample showed a reduction in these artifacts, leading to improved image quality. A more detailed analysis and evaluation, including algebraic filter parameters, will be presented and discussed at the conference.

ACKNOWLEDGEMENTS

This work was supported by the National Research Foundation of Korea (NRF) grant funded by the Korea government (MSIT) (RS-2024-00340520).

REFERENCES

[1] V.-G. Herminso et al., Assessing rechargeable batteries with 3D X-ray microscopy, computed tomography, and nanotogmography, Nondestructive Testing and Evaluation, Vol. 37, No. 5, pp. 519-535, 2022.
[2] N. Tirada et al., Digital breast tomosynthesis: Physics, artifacts, and quality control, Radiographics, Vol. 39, No. 2, pp. 412-426, 2019.
[3] Y.-C. Lai et al., Digital breast tomosynthesis: Technique and common artifacts, Journal of Breast Imaging, Vol. 2, No. 6, pp. 615-628, 2020.
[4] G. L. Zeng, Model based filtered backprojection algorithm: A tutorial, Biomedical Engineering Letters, Vol. 4, No. 1, pp. 3-18, 2014.